Exploring the Reactivity of Donor–Acceptor Systems through a Combined Conceptual and Constrained DFT Approach

Johanna Klein, Julien Pilmé

Exploring The Reactivity of Donor-Acceptor Systems Through a Combined Conceptual and Constrained DFT Approach

Johanna Klein [1] and Julien Pilmé* [1]

[1] Sorbonne Université, CNRS, Laboratoire de Chimie Théorique CC 137 – 4, place Jussieu F. 75252 PARIS CEDEX 05 – France.

ABSTRACT: In the context of the conceptual Density Functional Theory (cDFT) and based on the computational efficiency of the constrained DFT (CDFT), we demonstrate that chemical reactivity can be governed by the difference between the local interacting chemical potentials of the reactants (referred as E_{dual}), in agreement with the Sanderson's equalization principle. In a proof-of-concept study, we investigated illustrative examples involving typical non-covalent donor-acceptor systems as well as reactive systems are provided. For the selected systems, our approach reveals a significant mimicking between E_{dual} and the DFT-computed intermolecular interaction energy profiles. We further evaluate the influence of the coulomb and exchange-correlation contributions in E_{dual}. These latter results suggest that numerous potential energy surfaces of clusters can be explored using a Sanderson-like model only based classical interactions between molecular orbitals domains. To conclude, this study achieved a deeper understanding of the principles of cDFT and assessed, in a wider context, its efficiency in predicting the chemical reactivity.

1. Introduction. The development of rigorous and computationally usable methods to rationalize and predict the interactions within and between the molecules is a major purpose of theoretical chemistry. In this context, the Conceptual Density Functional Theory (cDFT) offers a comprehensive framework of tools for comprehending and predicting the electronic structure and the chemical reactivity of molecules and materials. [1-5] cDFT fundamentally hinges on the principle that the ground state energy of an N-electron system, as dictated by the Hohenberg-Kohn theorem, depends on the number of electrons (N) and the external potential, both of which are uniquely determined by the electron density.[6] In this framework, the system's response to changes in the number of its electrons or the external potential, gives valuable insights into its reactivity and provides a way to justify the reactivity principles in cDFT, such as the Sanderson's electronegativity equalization[4, 7-10], the Pearson's hard/soft acid-base (HSAB) principle[11, 12, 13-17], the maximum hardness and minimum electrophilicity rules[18,19, 20] , or the principle "|Δμ| big is good " also known as DMB rule.[21, 22]

Even when the external potential remains constant, the energy change (ΔE) can be defined in terms of the response to variations in the number of electrons ΔN. This latter energy is most of the time approximated by the quadratic Taylor expansion truncated after the second-order terms[9] :

$$\Delta E = E(N^{\circ} + \Delta N) - E(N^{\circ}) \approx \mu\,\Delta N + \eta\,\frac{\Delta N^2}{2} \qquad (1)$$

where $\mu = \left(\frac{\partial E}{\partial N}\right)_v$ and $\eta = \left(\frac{\partial^2 E}{\partial N^2}\right)_v$ are the electronic chemical potential and the chemical hardness, respectively and N^0 is the number of electrons of the relevant isolated system.[4, 23, 24]

From its beginning, a large part of the cDFT works have been focused on the electronic chemical potential, clearly identified in the above-mentioned Taylor expansion as the partial first derivative of the system's energy with respect to the number of electrons at fixed external potential *v*. However, its practical calculation requires an operational expression that must be readily computable from standard electronic structure calculations. In this context, the most commonly employed equations are typically carried out within the finite difference approach, in which it is calculated as the average of the left- and right-hand-side derivatives:

$$\mu^- = E(N^0) - E(N^0 - 1) = -I$$
$$\mu^+ = E(N^0 + 1) - E(N^0) = -A$$

where I and A are the vertical ionization energies and electron affinities of the N^0-electron system (neutral or charged)

$$\mu = \frac{\mu^- + \mu^+}{2} = \frac{E(N^0 + 1) - E(N^0 - 1)}{2} = -\frac{I + A}{2}$$

For atoms, the chemical potential has long been identified as negative electronegativity of Mulliken.[25]

$$\mu = -\frac{I + A}{2} = -\chi$$

Interestingly, the negative chemical potential closely follows the same trends in atoms as those obtained by Pauling.[26] Based on the definition of the electronegativity, identified as negative chemical potential, Sanderson has formulated its equalization principle.[7, 8] The correctness of Sanderson's principle relies on the variations of chemical potentials strongly linked to a property of an equilibrium state. The fact that the chemical potential is related to the Pauling's electronegativity and the fact that the chemical hardness reproduces the qualitative scales derived by Pearson[12] reinforces the identification of coefficients that one will find in the quadratic Taylor expansion with the corresponding chemical concepts. Overall, these coefficients provide an intrinsic response of the system to the attacking partner.[2, 4] A pivotal concept in cDFT is that derivatives represent a response of the system independent of other

reactants involved in the reaction, as well as certain effects of the molecular environment, such as solvent effects.[2, 27-30] It was proposed through a simple way to take into account the perturbations effects on the descriptors of a given species when it weakly interacts with another one. [27, 28, 30] For example, within the framework of the grand canonical ensemble, the definitions of the electronic chemical potential and the chemical hardness can be extended to finite temperatures by considering a reactive species as an open system to the exchange of electrons. [31, 32] The goal is to enhance the description of their chemical reactivity. The significance of such perturbed chemical potential can be further illustrated by examining its local version.[33, 34]. Let us consider the formation of a supermolecule MA-MB from the association of two molecules MA and MB. [26] When the two molecules MA and MB approach one another, there is a flux of electron density from the species with higher chemical potential towards the one with lesser chemical potential, in order to equilibrate the two chemical potentials in the new interacting system. As the reactants come closer, the external potential affecting one molecule undergoes changes due to the presence of the other reactant. This perturbation of the external potential forces the electron density to distort itself, adapting to the new electron density that corresponds to the updated chemical potentials Although this process is easily understandable, the practical computation of the such interacting chemical potentials and their link to the Sanderson's principle is still challenging and requires more detailed studies.[35, 36]

The present work addresses an original strategy designed to practically compute the interacting chemical potentials by combining on equal footing treatment between cDFT and the Contrained DFT approach. We aim to demonstrate that this combined approach can be quantitatively used to predict not only the minima but also to provide the shape of the energy profile from reactants to the transition state. An essential objective of this proof-of-concept study is to evaluate its effectiveness in predicting reactivity in a broader and more quantitative context. Additionally, the results presented in this contribution seeks to enhance our understanding of the efficacy of a model approach based on the E_{dual} calculation, which we had initially proposed in the narrower context of quantum chemical topology .[37, 38]

2. The E_{dual} quantity. Turning to the smooth quadratic Taylor expansion that results in the change in the energy due to the electron transfer between the two subsystems MA and MB [6, 11, 39, 40] :

$$\Delta E_{MAMB} \approx \left[\left(\frac{\partial E}{\partial N_A}\right)_{N_B} - \left(\frac{\partial E}{\partial N_B}\right)_{N_A}\right]\Delta N_A + \left[\left(\frac{\partial^2 E}{\partial N_A^2}\right)_{N_B} + \left(\frac{\partial^2 E}{\partial N_B^2}\right)_{N_A} - 2\left(\frac{\partial^2 E}{\partial N_A \partial N_B}\right)\right]\frac{\Delta N_A^2}{2} \qquad (2)$$

In which we used that the total variation of electrons $\Delta N = \Delta N_A + \Delta N_B = 0$ because the total system is isolated. By identifying Equation (2) to Equation (1), the local chemical potentials[33] of the interacting reactants MA and MB can be defined as $\mu_{MA} = \left(\frac{\partial E}{\partial N_A}\right)_{N_B}$ and $\mu_{MB} = \left(\frac{\partial E}{\partial N_B}\right)_{N_A}$.

So that the small changes in the total energy can be directly related to the interacting chemical potentials at the first-order variation by:

$$\Delta E_{MAMB} \approx (\mu_{MA} - \mu_{MB})\, \Delta N_A \quad (3)$$

Additionally, in a reaction path where two molecular reactants MA and MB approach each other, the intermolecular interaction energy E^{int} between MA and MB can be also obtained from a supermolecular point of view:

$$E_{MAMB} = E^{int} + E^{0}_{MA} + E^{0}_{MB}$$

where E is the total energy of the MA--MB supermolecule, and E^0_{MA} and E^0_{MB} correspond to the energies of reactants calculated in their relevant isolated states, respectively. Thus,

$$\mu_{MA} = \left(\frac{\partial E}{\partial N_A}\right)_{N_B} = \left(\frac{\partial E^{int}}{\partial N_A}\right)_{N_B} + \left(\frac{\partial E^{0}_{MA}}{\partial N_A}\right)_{N_B} + \left(\frac{\partial E^{0}_{MB}}{\partial N_A}\right)_{N_B} \quad (4)$$

Since $\left(\frac{\partial E^0_{MB}}{\partial N_A}\right)_{N_B} = 0$ and $\mu^{\circ}_{MA} = \left(\frac{\partial E^0_{MA}}{\partial N_A}\right)_{N_B}$

$$\Delta E_{MAMB} \approx \left[\left(\frac{\partial E^{int}}{\partial N_A}\right)_{N_B} - \left(\frac{\partial E^{int}}{\partial N_B}\right)_{N_A} + \mu^{\circ}_{MA} - \mu^{\circ}_{MB}\right] \Delta N_A = (\mu_{MA} - \mu_{MB})\, \Delta N_A \quad (5)$$

In previous works[37, 38], a relationship between cDFT and Quantum Chemical Topology (QCT) was explored by computing the first-order variation of the coulomb intermolecular interaction energy with respect to the number of electrons from interacting domains of the modified electron localization function ELF_x.[41] In the context, this variation was defined as E^{Coul}_{dual} :

$$E^{Coul}_{dual} = \left(\frac{\partial E^{int}_{coul}}{\partial N_A}\right)_{N_B} - \left(\frac{\partial E^{int}_{coul}}{\partial N_B}\right)_{N_A}$$

According to Eq. (5), E_{dual} can be extended beyond its sole coulomb contribution as follows :

$$E_{dual} = \left(\frac{\partial E^{int}}{\partial N_A}\right)_{N_B} - \left(\frac{\partial E^{int}}{\partial N_B}\right)_{N_A} = \mu_{MA} - \mu_{MB} - (\mu^{\circ}_{MA} - \mu^{\circ}_{MB}) = (\mu_{MA} - \mu^{\circ}_{MA}) - (\mu_{MB} - \mu^{\circ}_{MB})$$
$$= \Delta\mu_{MA} - \Delta\mu_{MB} \quad (6)$$

ΔE_{MAMB} is stabilising (negative) when $(\mu_{MA} - \mu_{MB})$ and ΔN_A are opposite sign. In this approach, the chemical potentials of each interacting fragments differ when the interaction energy between MA and MB changes. Equation (5) clearly remains a reasonable approximation for a typical association reaction MA + MB $\longrightarrow$ MA--MB where geometries of reactants and transition state remains close, one can neglect the change of the external potential. Overall, in a chemical reactive process, the electronegativity equalization principle, indicate that the electron transfer between subsystems should continue until their relative electronegativity values become equal. From Equation (6) this means that E_{dual} goes the minimal limit $-\left(\mu^{\circ}_{MA} - \mu^{\circ}_{MB}\right)$ at the equilibrium. Therefore a large $-\left(\mu^{\circ}_{MA} - \mu^{\circ}_{MB}\right)$ should be linked to a large interaction energy between the reactants. We recover here the rule "|Δμ| big is good " already postulated by Parr and Yang thirty years ago.[22, 42] In contrast, when MA and MB are located far from each other, $\mu_{MA/MB} \rightarrow \mu^{\circ}_{MA/MB}$ and E_{dual} goes to zero. Interestingly, a mimicking of E_{dual} onto the interaction energy can thus be expected. Note that some of us have proposed a way to compute the E_{dual} quantity based on the interacting quantum chemical topology domains. [37]

3. Computational Details.

3.1 Constrained DFT (CDFT). In this article, we assume that the reader is familiar with the CDFT method because numerous presentations of the methodology and many applications have already been published in the literature. [43-46] Briefly, CDFT computes diabatic states for charge transfer reactions typically using the KS-DFT formalism. CDFT allows the accurate calculation of charge transfer phenomena in a quantitative way and it was widely used not only in charge transfer mechanisms but also in chemical reactivity, applied to ground states, excited states and to compute the barrier heights. The CDFT framework was proposed for solving the electronic structure of any molecular system within the following constraint on the electron density:

$$\theta = \int w(\boldsymbol{r})\, \rho(\boldsymbol{r}) d\boldsymbol{r} - N = 0$$

N is the targeted population (computed in electrons) depending on weight functions $w(\mathbf{r})$ that define the constraint. This latter is directly related to the partition of the molecular space used to define the subsystem in the supermolecule. The constrained lowest-energy state can be obtained from an optimization problem via the standard method of Lagrange multipliers.[47]

$$\underbrace{min}_{\rho}\underbrace{max}_{\lambda}\left(E_{DFT}+\lambda\,\theta\right)$$

Herein, E_{DFT} is the DFT energy and λ is the Lagrange multiplier. The constrained electron density deviates from the constraint-free adiabatic ground-state density, making it a typical diabatic state. The weight functions depend on the partitioning of the electron density within the complex and on how electrons are assigned to the molecular fragments. Within the software *Q-Chem*, the weights are built as a linear combination of the Becke's atomic partitioning functions in which a set of empirical atomic radii are used.[48, 49] The summation runs over the atoms and the spin within the system. The weight function is designed to be close to one near a given atom and falls to zero near any other atom in the system.

3.2 Level of Theory. The B3LYP hybrid functional level with the QChem5.4 software was used for all calculations of total and intermolecular interaction energies.[50] The standard all-electron cc-p-VDZ was used for all atoms except for the CuCO complex, where the TZV basis set was used. The empirical dispersion correction D3-BJ of Grimme[51] has been employed for the benzene dimer system since the dispersions effects need to be taken into account. The empirical atomic radii of Bragg-Slater have been used for the Becke's partition scheme used in the constrained DFT calculations.[48]

4. Practical Computation of local interacting chemical potentials

The CDFT diabatic energies such as $E\left(N_{MA}^{\circ}+1,N_{MB}^{\circ}\right)$ constraints the $\left(N_{MA}^{\circ}+1\right)$ population (and th corresponding spin) within the MA fragment defined by the Becke's scheme and N_{MB}° population in the MB fragment, N_{MA}° and N_{MB}° being the total population of the isolated molecules, MA and MB being respectively calculated in their relevant isolated states. For example, $E\left(N_{MA}^{\circ}+1,N_{MB}^{\circ}\right)$ is the total energy when the MA fragment vertically ionized ($N_{MA}^{\circ}\rightarrow N_{MA}^{\circ}+1$) and the fragment MB interacts. Thus, within the finite difference approach, the interacting chemical potential of the donor μ_{MA} can be defined as follows,

$$\mu_{MA}\approx\frac{E\left(N_{MA}^{\circ}+1,N_{MB}^{\circ}\right)-E\left(N_{MA}^{\circ}-1,N_{MB}^{\circ}\right)}{2}$$

and similarly for the acceptor,

$$\mu_{MB} \approx \frac{E\left(N_{MA}^{\circ}, N_{MB}^{\circ}+1\right) - E\left(N_{MA}^{\circ}, N_{MB}^{\circ}-1\right)}{2}$$

In these two latter expressions, the energy remains a function of the number of electrons which is a piecewise quantity comprised by straight lines joined at integer number of electrons. To practically compute the CDFT diabatic energies, the applied charge constraint is designed to preserve the Becke's charges found in the isolated fragments used here as a reference. For instance, the chemical potential μ_{MA} is computed by evaluating the diabatic energies $E\left(N_{MA}^{\circ}, N_{MB}^{\circ}+1\right)$ and $E\left(N_{MA}^{\circ}, N_{MB}^{\circ}-1\right)$, where the Becke's charges of fragment MA have been constrained to those found in the isolated corresponding fragment. This enables to roughly frozen the electron density within a specified fragment, which is essential since it has been shown that the contribution of such frozen density to the total energy is dominant, while those of polarization and charge transfer remain small.[52] Even though it has been shown that Becke's partition may not the most suitable for computing a physically sound charge transfer between molecular fragments[53], the calculation of interacting chemical potentials essentially requires to maintain the charges distribution found in the targeted isolated fragment. For the dative systems, the metal-ligand interactions and the reactive systems where the charge transfer can increase, a spin constraint has also been applied in addition to the charge constraint.

Finally, E_{dual} computed within the CDFT context is the difference between the interacting chemical potentials defined as follows,

$$E_{dual}^{FD} \approx \frac{E\left(N_{MA}^{\circ}+1, N_{MB}^{\circ}\right) - E\left(N_{MA}^{\circ}-1, N_{MB}^{\circ}\right) - E\left(N_{MA}^{\circ}, N_{MB}^{\circ}+1\right) + E\left(N_{MA}^{\circ}, N_{MB}^{\circ}-1\right)}{2} - \left(\mu_{MA}^{\circ} - \mu_{MB}^{\circ}\right) \quad (7)$$

Equation (7) should be reasonably accurate for all non-covalent interactions (hydrogen bonds, halogen bonds, VdW, etc..) or at the beginning of the chemical reaction paths where the charge transfer from the donor to the acceptor remains enough small. In the paper, we explore the ability of Equation (7) to describe and to predict the topology of the potential energy curves including its relevance when the chemical reactivity potentially involve other interactions. Two selected examples have been explored through a typical S_N2 mechanism and for a Diels Alder mechanism.

5. Applications to the Chemical Reactivity

5.1 **Selected Systems**. In principle our methodology can be applied to any system or chemical reaction where a charge transfer occurs from a donor to an acceptor moieties. Overall, we explored the conformational space of the interacting fragments MA (donor) + MB (acceptor) → MA--MB, seeking minima and maxima on the potential energy curves of E_{dual}^{FD} using the constrained DFT methodology. For all selected systems, we do not disregard that the calculation of E_{dual} is related to small changes in the total energy computed at the first-order variation when the external potential $v(\mathbf{r})$ remains constant (Equation (3)). This implies that geometries of reactants and transition state need to remain close, so that we can neglect the change of the external potential. As shown in Figure 1, we review some examples where the applicability of E_{dual} has been evaluated. First, we considered bounded by non-covalent interactions: the benzene dimer and a typical hydrogen bond FH—CO/OC. Dative bond schemes for $N_2 + BH_3 \rightarrow N_2BH_3$ for the formation of borazane $NH_3 + BH_3 \rightarrow NH_3BH_3$ and for the metal-ligand interaction Cu (^2S) + CO ($^1\Sigma^+$)→ CuCO ($^2A'$) have then been considered. Thereafter, we have considered two reactive processes with the well-known example of the S_N2 reaction $Cl^- + CH_3Cl \rightarrow CH_3Cl + Cl^-$ and for the classical Diels Alder mechanism $C_2H_4 + C_4H_6$ → Cyclohexene which remains a subject of intensive studies. For non-covalent and weak donor-acceptor systems the geometries of fragments have been frozen and maintained to their isolated geometry in all calculations.

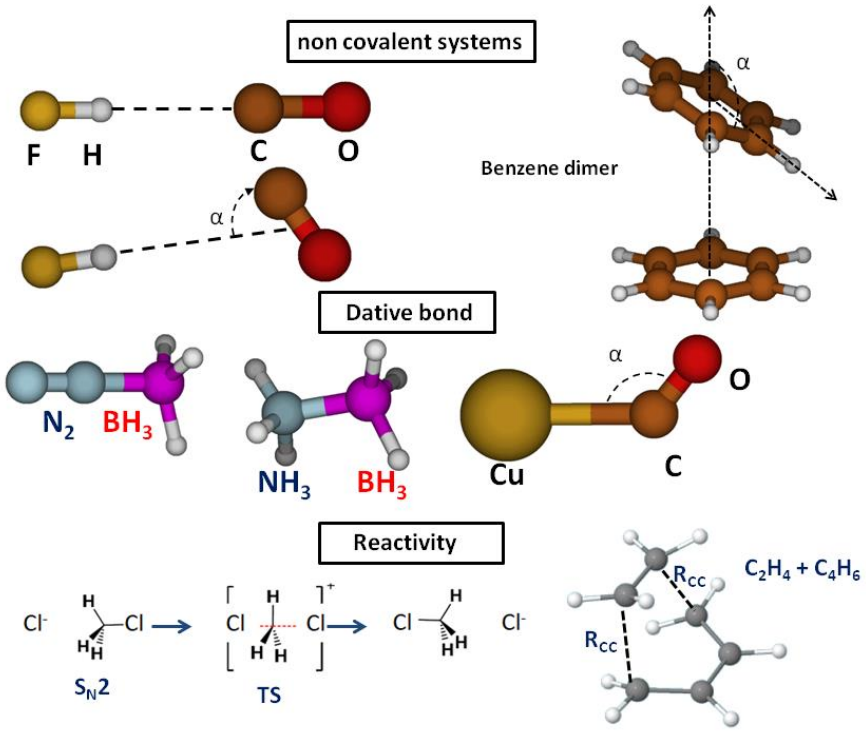

Figure 1. Selected Systems

For clarity and the tractability of the data analysis, all the provided curves have been displayed as normalized plots $\frac{f-min\,(f)}{max(f)-min\,(f)}$ where f is the studied function namely f ≡ interaction energy or f ≡ E_{dual}^{FD}.

5.2 Results and Discussion

5.2.1 Non-covalent Interactions. Let us consider the case of typical non-covalent systems for which the charge transfer between monomers is expected to be small and the geometries of reactants and transition state remain close. We begin with the hydrogen bonding scheme. Numerous theoretical and experimental studies on the nature and the strength of hydrogen bonds (HB) can be found in the scientific literature, which testifies to the importance of this donor-acceptor interaction scheme in any field in chemistry and in biology. Thus, efforts to better understand HB interactions remain of interest. For example, the case weakly bound dimer complexes FH--CO and FH--OC both of them are associated with a minimum, FH--CO being the most stable complex.[54] Figure 2 displays two comparative studies of the variation of E_{dual}^{FD} v.s. the DFT intermolecular interaction energy. The first one describes the rotation of CO around the center of mass of the FH molecule (see Figure 1). The second study describes the formation process FH ($^1\Sigma^+$) + CO ($^1\Sigma^+$) → FH--CO ($C_{\infty v}$).

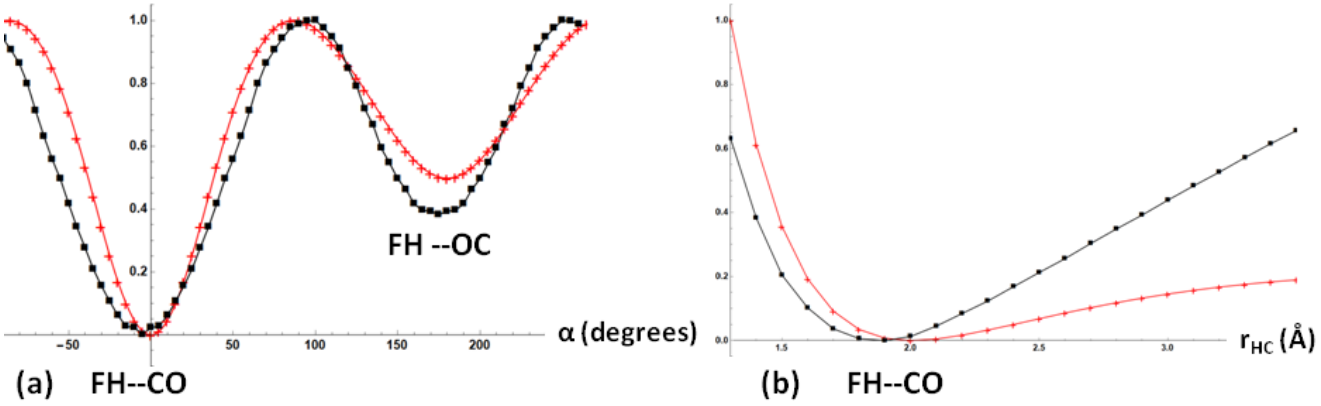

Figure 2. Comparative study of the normalized variation of E_{dual}^{FD} (black) v.s. the DFT intermolecular interaction energy (red). The orientation of monomers is displayed in Figure 1 (a) Rotation of the CO species around the FH molecule (mass centers of reactants separated from 3 Å) calculated at the B3LYP/cc-pVDZ level of theory. (b) FH + CO → FHCO energy surface calculated at the B3LYP/cc-pVDZ level of theory as a function of the C-H distance (Å). The geometries of reactants is constrained to that obtained in their isolated states (see Figure 1).

Figure 2 (a) illustrates that E_{dual}^{FD} closely aligns with the DFT curve, particularly the nearly identical location of critical points. Indeed, we observe two minima for α = 0° (FHCO) and α = 180° (FHOC) whereas a maximum is observed for α = 90° (the CO fragment is perpendicular to the FH fragment). It highlights an

excellent mapping of E_{dual}^{FD} and the DFT intermolecular interaction energy. Hence, Figure 2 (b) displays the E_{dual}^{FD} profile for the formation of FHCO, notably the location of the global minima (around 2 Å). Again, E_{dual}^{FD} appears in excellent agreement with the DFT profile.

Another example of non-covalent system is the forming benzene dimer which is an interesting system for evaluated our methodology when it comes to studying non-covalent interactions where the dispersion effects can be large.[55] Numerous theoretical as well as experimental studies showed that two main stable structures are competitive with each other (each of them being part of the S22 database[56]: the T-shaped dimer where the two cycles are perpendicular to each other, with one hydrogen pointing towards the center of the other cycle and the parallel displaced dimer where the two cycles are parallel but slightly offset from each other (see Figure 1). The first experiments, which concluded that it was a polar dimer, initially suggested that it was in a T-shaped conformation. It wasn't until the early 1990s with the first Raman spectroscopic analyses that it was shown that the benzene dimer existed in two different forms, one with a higher degree of symmetry than the other. In this section, we explore the geometries around the stable planar displaced conformation, examining the rotation of the C_6H_6 monomers around the minima associated with the planar displaced structure, as depicted in Figure 1. Figure 3 displays this comparative study of the variation of E_{dual}^{FD} v.s. the DFT intermolecular interaction energy.

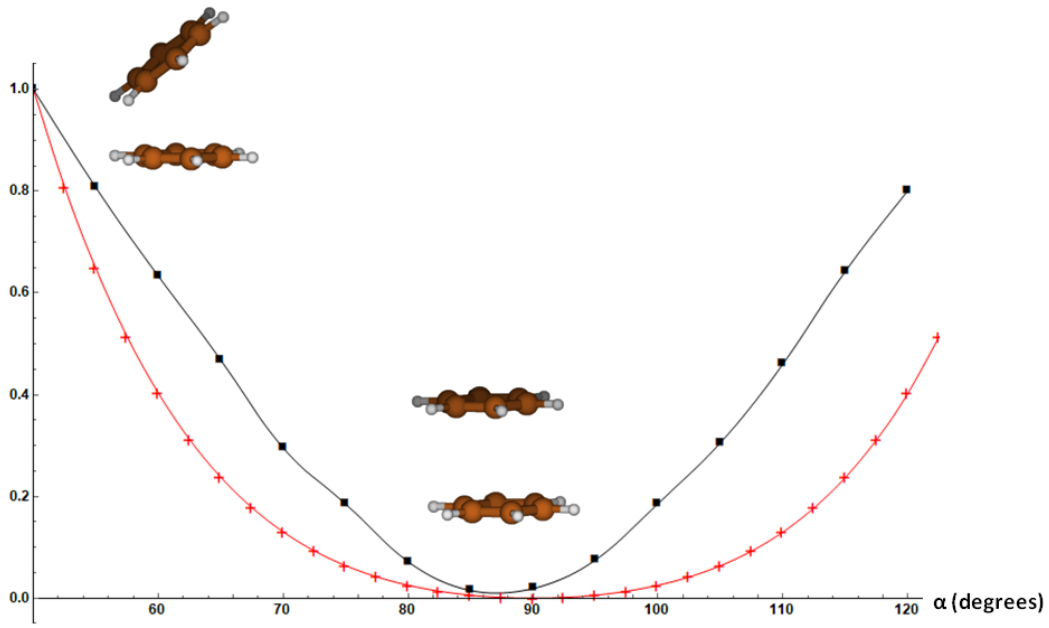

Figure 3. Comparative study of the normalized variation of E_{dual}^{FD} (black) vs the DFT intermolecular interaction energy (red) for the benzene dimer calculated at the B3LYP-D3/cc-pVDZ level of theory as a function of the angle between the two monomers C_6H_6. Each monomer is frozen in the geometry of the isolated states (see Figure 1). The distance between the ring centers is frozen to 3.6 A.

Once more, as shown in Figure 3, E_{dual}^{FD} corresponds closely to the DFT curve for some geometries associated to the rotation of monomers around the stable planar displaced conformation. Notably, we observe an almost identical location of the minimum ($\alpha = 90°$) given by both E_{dual}^{FD} and the DFT.

5.2.2 Dative bond. Let us consider the case of the formation of the BH_3N_2 and BH_3NH_3 molecules. The BH_3N_2 complex is known as a weak dative bond system.[57] The equilibrium structure exhibits a short B—N distance near 1.60 Å quite comparable to that of a strong acid—base complex like borazane $H_3N—BH_3$. However, its binding energy is lower than 6 kcal/mol. The chemical path of BH_3NH_3 has long been known: Fujimoto et al.[58] determined in 1974 that the covalent bond formation comes from a well-known strong electron transfer between the HOMO of NH_3 and the LUMO of BH_3 as an archetypical strong Lewis acid/base mechanism where the charge transfer from NH_3 to BH_3 is large. The robustness of our methodology was evaluated for these two reaction paths. We then explored the conformational space and we looked for the minima on the potential energy curve of E_{dual}^{FD}. Figure 4 displays a one-dimensional profile of E_{dual}^{FD}.

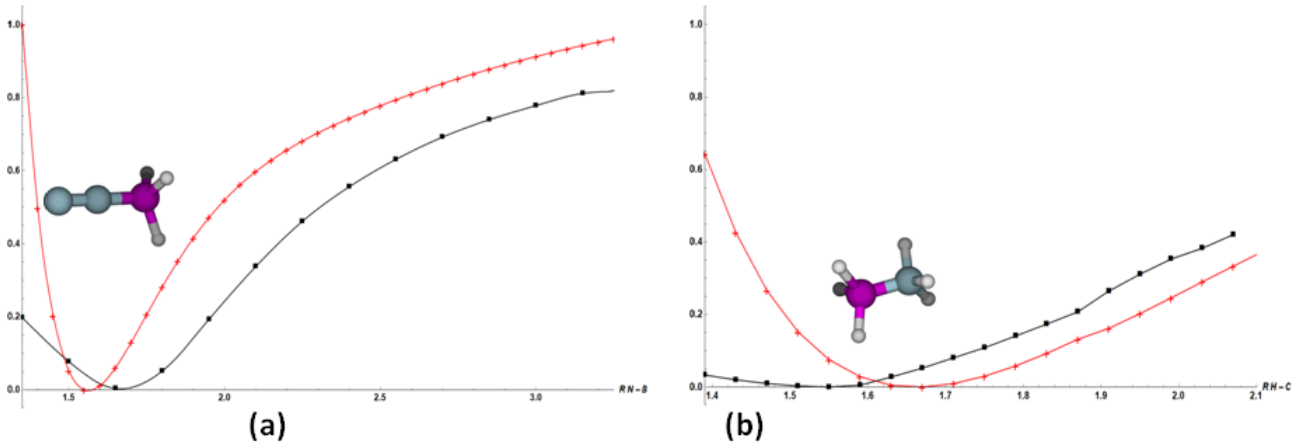

Figure 4. Comparative study of the normalized variation of E_{dual}^{FD} (black) vs the DFT intermolecular interaction energy (red). (a) N_2 (donor) + BH_3 (acceptor) → N_2-BH_3; (b) NH_3 (donor) + BH_3 (acceptor) → NH_3-BH_3. All calculations at the B3LYP/cc-pVDZ level of theory as a function of the N-B distance. The curves correspond to constrained geometries of reactants in their isolated states.

We observe a noticeable mapping of E_{dual}^{FD} onto the intermolecular interaction energy plot. First of all, the weak dative scheme given by E_{dual}^{FD} for BH_3N_2 strongly agrees with DFT intermolecular interaction energy since the expected minima between N_2 and the Lewis-base BH_3 (Figure 4 a) is clearly identified on the curve at almost the same location (1.60 Å for E_{dual}^{FD} vs 1.55 Å for DFT). Regarding the borazane, the location of the minima slightly differs between E_{dual}^{FD} (1.55 Å) and the

interaction energy (1.65 Å) as observed on Figure 4 b. This indicates that E_{dual}^{FD} l is less accurate for short distances because the charge transfer increases.

5.2.4 Metal-Ligand interactions. The interaction between transition-metal atoms and CO is of significant interest as a fundamental model for both molecular and surface chemistry. Among small transition-metal complexes, metal-monocarbonyls, M-CO have been subject to numerous theoretical investigations in particular the complex CuCO (^{2}A). [59, 60] A noticeable point for this latter structure is his bent geometry (C_s symmetry) whereas other M-CO complexes are linear. DFT calculations showed that the linear Cu-CO corresponds to a transition state.[61] The stabilization energy ranges from a few kcal/mol to a typical donor – acceptor bonding scheme. Therefore, it is an interesting to challenge the E_{dual}^{FD} methodology demonstrating its ability to characterize this bent structure. Figure 5 shows two comparative studies of E_{dual}^{FD} vs DFT. The first one (Figure 5a) reports the curves for the reaction CO + Cu → CuCO whereas the second one (Figure 5 b) gives the rotation of CO around Cu (see Figure 1). We used a time-tested process based on the frozen center of mass separation (3 Å) of CO and Cu and the rotation angle.

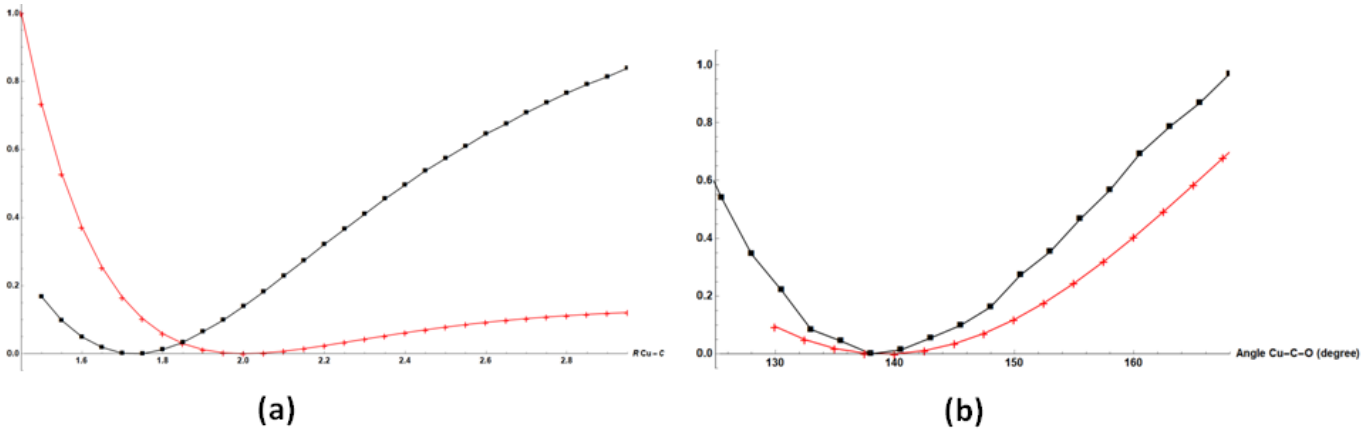

Figure 5. Comparative study of the normalized variation of E_{dual}^{FD} (black) v.s. the DFT intermolecular interaction energy (red) (a) CO (donor) + Cu (acceptor, ^{2}A) → CuCO calculated at the B3LYP/TZV level of theory as a function of the Cu-C distance. (b) Rotation of the CO species around Cu (calculated at the B3LYP/TZV level of theory The curves correspond to a constrained geometries of reactants in their isolated states.

Up to now most descriptions of the bonding of the metal-CO complexes, rely on the traditional picture of Dewar, Chatt, and Duncanson (DCD) model based on a balance between σ donation from the carbonyl (the carbon lone pair) to the vacant orbital of the metal atom and π back-donation from the metal to the CO π* orbital. [62] By definition, E_{dual}^{FD} takes into account both the donation and the back-donation schemes. As shown in Figure 5 a, the profile of E_{dual}^{FD} obtained for the reaction Cu + CO → CuCO mimicks well the DFT curve in particular the minima between CO and the copper atom

is clearly identified on the both curves even if the location of minima differs (1.70 Å for E_{dual}^{FD} vs 2.0 Å for DFT). This could explained by the relatively large variation of the total charge transfer (donation + back-donation) upper than 0.2 electron between Cu and CO when the RCu-C distance approaches of the equilibrium distance (around 1.9 Å).[59] In the latter case, E_{dual}^{FD} is expected to be less accurate in this short distances regime because the charge transfer increases. For the comparative studies where the Cu-C-O angle (Figure 5 b) gradually increases from 130° to 160°, the E_{dual}^{FD} and DFT plots are almost in perfect agreement showing a minimum for the bent structure (Cu-C-O angle of 139°).

5.2.5 Chemical Reactivity

The S_N2 reactivity : $Cl^- + CH_3Cl$

The determination of chemical processes for a given chemical rearrangement is an issue of major concern. The usual approach toward the quantum mechanical representation of chemical reactions is based on the evolution of the energy profile along the channel connecting the reactants to products. For associative reactions (A + B → AB) involving non-covalent interactions, the methodology E_{dual}^{FD} is expected to predict the profiles of the intermolecular interaction energy, especially at long distances where the coulomb contribution largely predominates in the interaction between reactants. When the interaction between fragments MA and MB begins, E_{dual}^{FD} should be able to account for the overall behavior of the interaction energy variation, gradually decreasing until the observed minimum at the equilibrium distance where the chemical potentials of the reactants tend to equalize. Our results clearly demonstrate that non-covalent interactions can be adequately described by this methodology, thus, it is tempting to extend this work to interactions where the covalent component can become significant. We first consider the case of a second-order nucleophilic substitution (S_N2), a one-step chemical reaction during which a transition state, characterized by a saddle point on the potential energy surface, is formed. However, the first step of such a reaction may correspond to the formation of a pre-reactive complex formed by weakly bound reactants. This is a tetrel bond, which can involve all elements of Group IV.[63] As illustrated in Figure 1, we propose to address an archetype of S_N2 reactivity with the reaction pathway $Cl^- + CH_3Cl \rightarrow ClCH_3 + Cl^-$. The purpose of this section is to explore the applicability of our methodology to such reactions. The polarization of the Cl-C bond in the reactant leads to a depletion of charge density at the sp^3 hybridized carbon along the extension of this Cl-C bond, creating a σ-hole. The fluoride ion, due to its excess charge density, can then interact with this hole and form a σ-bond with the carbon.

This step can lead to the stabilization of a pre-reactive complex Cl-CH_3, which then starts the reaction towards the transition state. Figure 6 displays a comparative profile E_{dual}^{FD} vs DFT.

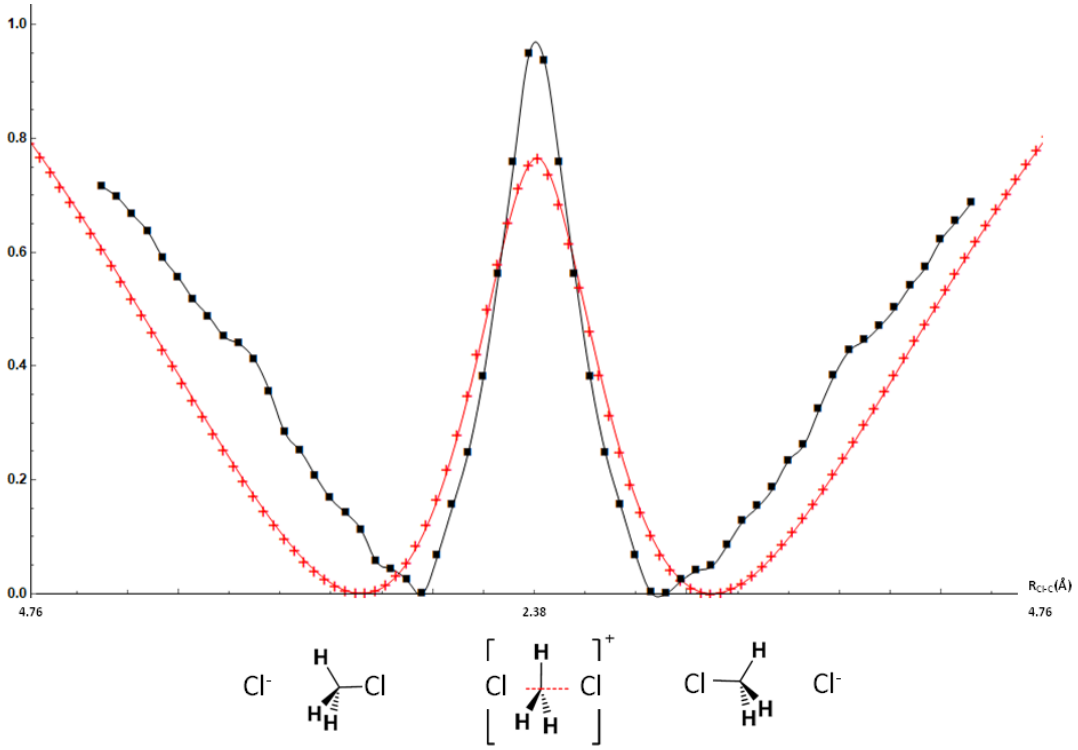

Figure 6. Comparative study of the normalized variation of E_{dual}^{FD} (black) vs the DFT intermolecular interaction energy (red) for the S_N2 reaction Cl^- + CH_3Cl calculated at the B3LYP/cc-pVDZ level of theory on geometries along the IRC.

At long distances, the E_{dual}^{FD} detects the formation of the tetrel bond Cl^-●●●CH_3Cl where the fragments are gradually brought closer together, E_{dual}^{FD} forms a minimum associated with the pre-reactive complex at an equilibrium distance dCl−C ≈ 2.82 Å. This distance is close enough to the DFT reference value of 3.06 Å. In addition the E_{dual}^{FD} profile gradually rises to a maximum observed at a distance d_{Cl-C} ≈ 2.38 Å. The profile then logically decreases again. These results clearly demonstrate that E_{dual}^{FD}, in the constrained DFT framework is able to describe and predict a mechanism involving the formation or breaking of bonds beyond the non-covalent systems.

The Diels Alder (DA) reaction C_2H_4 + C_4H_6

Another example illustrating the presence of a kinetic barrier is the pericyclic concerted Diels-Alder reaction which has become one of the most widely used methods in synthetic organic chemistry for carbon-carbon bond formation.[64] It has also been central in the developments of theoretical models of pericyclic reactions. [65] In particular, the DA reaction between ethylene and 1,3-butadiene to yield

cyclohexadiene is often taken as the textbook example of a pericyclic reaction.[66, 67] Figure 7 shows a comparative study of the normalized variation of E_{dual}^{FD} vs DFT following the R_{CC} distance (see Figure 1)

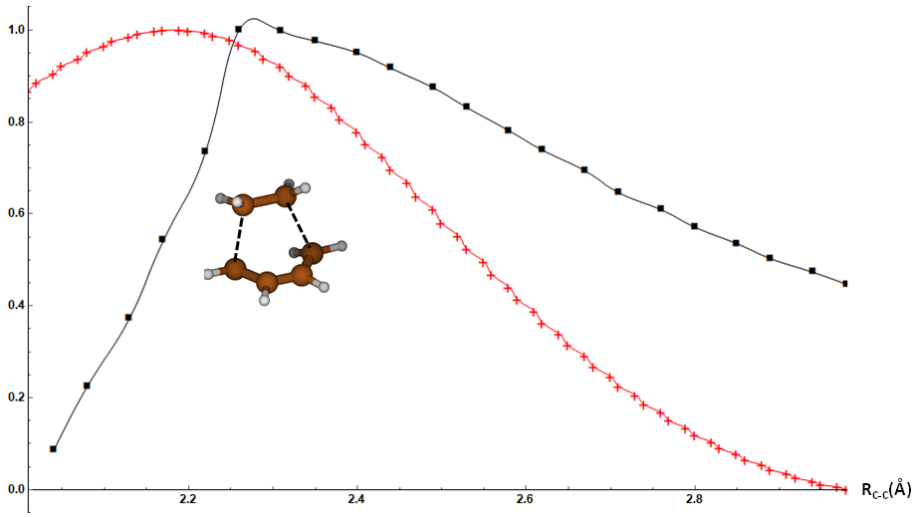

Figure 7. Comparative study of the normalized variation of E_{dual}^{FD} (black) v.s. the DFT intermolecular interaction energy (red) for the Diels-Alder reaction C_2H_4 + C_4H_6 calculated at the B3LYP/cc-pVDZ level of theory as a function of the R_{CC} coordinate.

The challenge in this study lies in testing whether the methodology can accurately replicate the activation barrier. As shown on Figure 7, E_{dual}^{FD} closely aligns with the DFT curve which gradually rises from the large distances R_{CC} to a saddle-point observed for E_{dual}^{FD} at $R_{Cl-C} \approx 2.3$ Å. This latter distance is very close to the DFT value of 2.2 Å. These results unequivocally illustrate that E_{dual}^{FD}, computed within the constrained DFT framework, aptly describes and predicts a chemical process that encompasses a transition state, extending beyond a straightforward associative process like MA-MB, which does not involve any kinetic.

6. Basis sets and DFT functional Dependence. A crude analysis of the dependence of E_{dual}^{FD} on the choice of the basis set and the employed DFT functional (Figures S1-S8) has been conducted to enhance our understanding of computational results. Illustrative examples for FHCO and NH_3BH_3 are provided in supplementary information. Once the basis set is sufficiently large to describe the system well (cc-pVDZ or cc-pVTZ), the profiles of E_{dual}^{FD} are well reproduced by the three selected functionals (PBE (GGA), rev-TPSS (meta-GGA) , wB97X-D3 (hybrid GGA)) and even at the Hartree-Fock level of theory. Despite small observed differences, the profiles of E_{dual}^{FD} are reasonably well reproduced regardless of the basis set, including the Pople-style basis set 6-31G(d, p). For FHCO, the best agreement between E_{dual}^{FD} and the DFT interaction energy is achieved at the B3LYP/cc-pVQZ level of theory. In the case of the formation of BH_3NH_3, the previously observed noticeable discrepancy between the minima location obtained from

E_{dual}^{FD} and the DFT interaction energy is consistently noted, irrespective of the DFT functional or basis set employed.

7. About energy contributions of chemical potentials. It has long been well-known that the electrostatic contributions account for a large fraction of the interaction energy for most intermolecular and non-covalent interactions even though other contributions are not necessary negligible or very small. In the context of this work, it is interesting to quantify the role and the magnitude of the diabatic DFT energies contributions involved in the calculation E_{dual}^{FD}. In DFT, it is customary to express the total energy functional, $E[\rho]$ as a combination of other functionals with well-defined physical and chemical meaning. Here, we consider a possible way to perform such decomposition : $E[\rho] = KE[\rho] + E_{coul}[\rho] + E_{XC}[\rho]$ where $KE[\rho]$ is the non-interacting kinetic energy, $E_{XC}[\rho]$ is the exchange–correlation energy, and $E_{coul}[\rho]$ is the classical coulomb energy. The latter can be further decomposed into the electron-nuclear interaction energy, the classical component of the electron–electron interaction and the nuclear-nuclear interaction energy. In a same way, the diabatic energies $E\left(N_{MA}^{\circ} \pm 1, N_{MB}^{\circ} \pm 1\right)$ and thereafter, E_{dual}^{FD}can be decomposed as follows :

$$E_{dual}^{FD} = E_{dual}^{FD,KE} + E_{dual}^{FD,coul} + E_{dual}^{FD,XC} \qquad (8)$$

Where , $E_{dual}^{FD,KE}$ is the kinetic energy part, $E_{dual}^{FD,coul}$ is the total coulomb contribution and $\mathrm{E}_{\mathrm{dual}}^{\mathrm{FD,XC}}$ is the total exchange-correlation contribution. For example, $\mathrm{E}_{\mathrm{dual}}^{\mathrm{FD,coul}}$ only involves the total coulomb contributions of constrained DFT energies $E\left(N_{MA}^{\circ} + 1, N_{MB}^{\circ}\right)$, $E\left(N_{MA}^{\circ} - 1, N_{MB}^{\circ}\right)$, $E\left(N_{MA}^{\circ}, N_{MB}^{\circ} + 1\right)$ and $E\left(N_{MA}^{\circ}, N_{MB}^{\circ} - 1\right)$. We select different systems previously studied. Figures 8 and 9 display the evolution of $\mathrm{E}_{\mathrm{dual}}^{\mathrm{FD}}$ without the exchange-correlation terms.

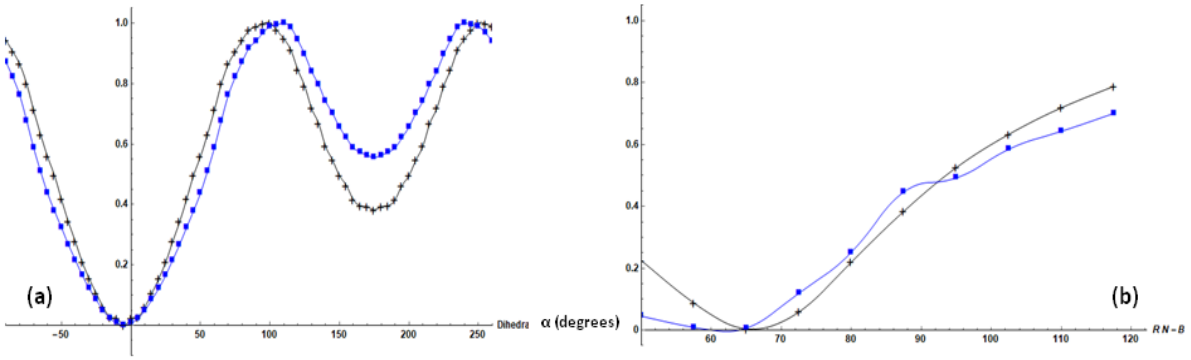

Figure 8. (a) Comparative study of the normalized variation of $E_{dual}^{FD,coul} + E_{dual}^{FD,KE}$ (blue) vs total E_{dual}^{FD} (black). (a) Rotation of the CO species around the FH molecule (mass centers separated from 3 Å) calculated at the B3LYP/cc-pVDZ level of theory.

(b)) N_2 (donor) + BH_3 (acceptor) → N_2-BH_3 , reaction process computed at the B3LYP/cc-pvdz level of theory according to the N-B constrained distance.

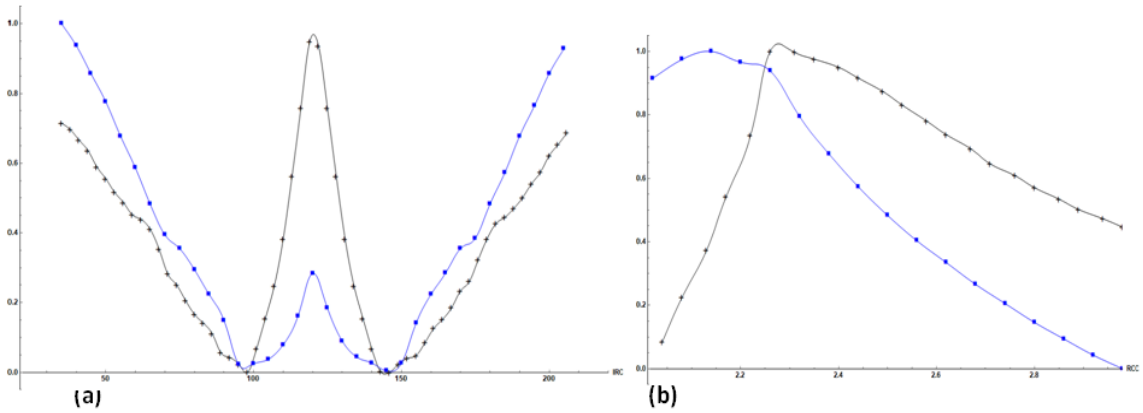

Figure 9. (a) Comparative study of the normalized variation of $E_{dual}^{FD,coul} + E_{dual}^{FD,KE}$ (blue) vs total E_{dual}^{FD} (black). (a) S_N2 reaction $Cl^- + CH_3Cl \rightarrow ClCH_3 + Cl^-$ calculated at the B3LYP/cc-pVDZ level of theory (b) Diels-Alder reaction $C_2H_4 + C_4H_6 \rightarrow$ Cyclohexene calculated at the B3LYP/cc-pVDZ level of theory.

The analysis of Figures 8 and 9 leads us to the following pithy comments: the curves of the sum $E_{dual}^{FD,coul} + E_{dual}^{FD,KE}$ (exchange-correlation contributions are disregarded) are quite comparable regardless of the system studied in this article. We particularly note that the locations of critical points (minima and maxima), appear in reasonable agreement with the total E_{dual}^{FD}. The results confirm that the coulomb potential and the kinetic energy account for a large fraction of the interaction energy whatever the donor-acceptor molecular system studied in this paper. $E_{dual}^{FD,coul}$ remains the driving term of the chemical reactivity when the two molecules interact. We can, however, note that the TS position for the Diels-Alder reaction has been approximatively shifted from a R_{CC} distance of 2.3 Å to a distance 2.1 Å, in better agreement with the DFT energy profile (see Figure 7). As these examples clearly confirm that the coulomb interaction largely contribute to the driving force of the intermolecular interaction between MA and MB, future works will focus on the fine-tuning simplified models of $\mathrm{E}_{\mathrm{dual}}^{\mathrm{FD,coul}}$ where the total coulomb interaction between the fragments will be particularly well addressed with, for example, the use of localized orbitals to properly describe the interaction between the reactants. The block-localized wavefunction (BLW, also known as extremely localized molecular orbitals) allows to define fragments with integer number of electrons even for the case of strongly interacting fragments as typically observed in transition states.[68] These localized orbitals will be used to improve $\mathrm{E}_{\mathrm{dual}}^{\mathrm{FD,coul}}$ for strongly interacting fragments, since they come together with orbital energies and are indeed strictly localized on the atoms of the fragment considered.

8. Concluding Remarks. By combining both the conceptual and the constrained DFT approaches, we proposed in a proof-of-concept study, an original point of view leading to an efficient scheme able to describe and predict the chemical paths. We have shown, in a rigorous way, how the first-order variation in the energy expressed in terms of the response to changes in the number of electrons where the external potential remains unchanged (interacting chemical potentials) can be a tractable quantity to drive the chemical reactivity between the reactants. Beyond non-covalent bonds, our methodology has also been tested with a S_N2 and a Diels-Alder mechanism showing kinetic barriers along the reaction path. For all systems, our approach unveils a noticeable mimicking of E_{dual} onto the DFT intermolecular interaction energy and we show that the global minima, but also structures higher in energy, can be clearly identified in order to predict the chemical reaction paths. For the S_N2 mechanism, E_{dual} effectively identifies the formation of the pre-reactive complex and traces the profile towards the transition state. Moreover, even when E_{dual} is restricted to its sole coulomb and kinetic contributions, it successfully describes the locations of the minima and the transition states in agreement with the results obtained in DFT. These latter results suggest that numerous potential energy surfaces of clusters can be explored using a Sanderson-like model only based classical interactions between molecular orbitals domains. To conclude, we note that this work has contributed to foster a deeper understanding of the principles of conceptual DFT and assessed its effectiveness in semi-quantitatively predicting chemical reactivity within a broader context.

AUTHOR INFORMATION. Corresponding Author
julien.pilme@sorbonne-universite.fr

Supporting Information
Additional comparative studies of the normalized variation of $\mathrm{E}_{\mathrm{dual}}^{\mathrm{FD}}$ v.s. the DFT intermolecular interaction energy are provided. Figure S1-S3 show results for different DFT functionals. Figure S4-S8 present results for B3LYP combined with different basis sets. This material is available free of charge via the Internet at http://pubs.acs.org.

ACKNOWLEDGMENT
We thank Dr. Frédéric Guégan and Pr. Paul Fleurat-Lessard for their critical reading of the manuscript and their constructive feedbacks.

REFERENCES

(1) Geerlings, P.; De Proft, F.; Langenaeker, W., Conceptual Density Functional Theory. *Chem. Rev.* **2003,** *103* (5), 1793-1874.
(2) Geerlings, P.; Chamorro, E.; Chattaraj, P. K.; De Proft, F.; Gázquez, J. L.; Liu, S.; Morell, C.; Toro-Labbé, A.; Vela, A.; Ayers, P., Conceptual density functional theory: status, prospects, issues. *Theor. Chem. Acc.* **2020,** *139* (2), 36.

(3) Calais, J.-L., Density-functional theory of atoms and molecules. R.G. Parr and W. Yang, Oxford University Press, New York, Oxford, 1989. IX + 333 pp. Price £45.00. *Int. J. Quantum Chem.* **1993,** *47* (1), 101-101.
(4) Parr, R. G.; Donnelly, R. A.; Levy, M.; Palke, W. E., Electronegativity: The density functional viewpoint. *J. Chem. Phys.* **1978,** *68* (8), 3801-3807.
(5) Iczkowski, R. P.; Margrave, J. L., Electronegativity. *J. Am. Chem. Soc.* **1961,** *83* (17), 3547-3551.
(6) Anderson, J. S. M.; Melin, J.; Ayers, P. W., Conceptual Density-Functional Theory for General Chemical Reactions, Including Those That Are Neither Charge- nor Frontier-Orbital-Controlled. 1. Theory and Derivation of a General-Purpose Reactivity Indicator. *J. Chem. Theory Comput.* **2007,** *3* (2), 358-374.
(7) Sanderson, R. T., Partial Charges on Atoms in Organic Compounds. *Science* **1955,** *121* (3137), 207-208.
(8) Sanderson, R. T., An Interpretation of Bond Lengths and a Classification of Bonds. *Science* **1951,** *114* (2973), 670-672.
(9) Parr, R. G.; Pearson, R. G., Absolute hardness: companion parameter to absolute electronegativity. *J. Am. Chem. Soc.* **1983,** *105* (26), 7512-7516.
(10) Parr, R. G.; Szentpály, L. v.; Liu, S., Electrophilicity Index. *J. Am. Chem. Soc.* **1999,** *121* (9), 1922-1924.
(11) Ayers, P. W.; Parr, R. G.; Pearson, R. G., Elucidating the hard/soft acid/base principle: A perspective based on half-reactions. *J. Chem. Phys.* **2006,** *124* (19).
(12) Pearson, R. G., Hard and Soft Acids and Bases. *J. Am. Chem. Soc.* **1963,** *85* (22), 3533-3539.
(13) Pearson, R. G., The HSAB Principle — more quantitative aspects. *Inorg. Chim. Acta* **1995,** *240* (1), 93-98.
(14) Miranda-Quintana, R. A.; Kim, T. D.; Cárdenas, C.; Ayers, P. W., The HSAB principle from a finite-temperature grand-canonical perspective. *Theor. Chem. Acc.* **2017,** *136* (12), 135.
(15) Pearson, R. G., Hard and soft acids and bases, HSAB, part 1: Fundamental principles. *J. Chem. Educ.* **1968,** *45* (9), 581.
(16) Pearson, R. G., Hard and soft acids and bases, HSAB, part II: Underlying theories. *J. Chem. Educ.* **1968,** *45* (10), 643.
(17) Ayers, P. W., An elementary derivation of the hard/soft-acid/base principle. *J. Chem. Phys.* **2005,** *122* (14).
(18) Miranda-Quintana, R. A.; Ayers, P. W., Note: Maximum hardness and minimum electrophilicity principles. *J. Chem. Phys.* **2018,** *148* (19).
(19) Pearson, R. G., Principle of Maximum Physical Hardness. *J. Phys. Chem.* **1994,** *98* (7), 1989-1992.
(20) Chattaraj, P. K.; Ayers, P. W., The maximum hardness principle implies the hard/soft acid/base rule. *J. Chem. Phys.* **2005,** *123* (8).
(21) Miranda-Quintana, R. A.; Ayers, P. W.; Heidar-Zadeh, F., Reactivity and Charge Transfer Beyond the Parabolic Model: the "|Δμ| Big is Good" Principle. *ChemistrySelect* **2021,** *6* (1), 96-100.
(22) Miranda-Quintana, R. A.; Heidar-Zadeh, F.; Ayers, P. W., Elementary Derivation of the "|Δμ| Big Is Good" Rule. *J. Phys. Chem. Lett.* **2018,** *9* (15), 4344-4348.
(23) Zhan, C.-G.; Nichols, J. A.; Dixon, D. A., Ionization Potential, Electron Affinity, Electronegativity, Hardness, and Electron Excitation Energy: Molecular Properties from Density Functional Theory Orbital Energies. *J. Phys. Chem. A* **2003,** *107* (20), 4184-4195.
(24) Parr, R. G.; Yang, W., Density functional approach to the frontier-electron theory of chemical reactivity. *J. Am. Chem. Soc.* **1984,** *106* (14), 4049-4050.
(25) Mulliken, R. S., A New Electroaffinity Scale; Together with Data on Valence States and on Valence Ionization Potentials and Electron Affinities. *J. Chem. Phys.* **2004,** *2* (11), 782-793.
(26) Pauling, L., THE NATURE OF THE CHEMICAL BOND. II. THE ONE-ELECTRON BOND AND THE THREE-ELECTRON BOND. *J. Am. Chem. Soc.* **1931,** *53* (9), 3225-3237.
(27) Miranda-Quintana, R. A.; Ayers, P. W., Fractional electron number, temperature, and perturbations in chemical reactions. *Phys. Chem. Chem. Phys.* **2016,** *18* (22), 15070-15080.
(28) Gázquez, J. L.; Cedillo, A.; Vela, A., Electrodonating and Electroaccepting Powers. *J. Phys. Chem. A* **2007,** *111* (10), 1966-1970.
(29) Pantoja-Hernández, M. A.; Franco-Pérez, M.; Miranda-Quintana, R. A.; Gázquez, J. L., Perturbed reactivity descriptors in the grand canonical ensemble. *Molecular Physics*, e2199105.
(30) Ayers, P. W.; Anderson, J. S. M.; Bartolotti, L. J., Perturbative perspectives on the chemical reaction prediction problem. *Int. J. Quantum Chem.* **2005,** *101* (5), 520-534.

(31) Franco-Pérez, M.; Ayers, P. W.; Gázquez, J. L.; Vela, A., Local and linear chemical reactivity response functions at finite temperature in density functional theory. *J. Chem. Phys.* **2015,** *143* (24).
(32) Franco-Pérez, M.; Gázquez, J. L.; Ayers, P. W.; Vela, A., Revisiting the definition of the electronic chemical potential, chemical hardness, and softness at finite temperatures. *J. Chem. Phys.* **2015,** *143* (15).
(33) Morell, C.; Ayers, P. W.; Grand, A.; Chermette, H., Application of the electron density force to chemical reactivity. *Phys. Chem. Chem. Phys.* **2011,** *13* (20), 9601-9608.
(34) Morell, C.; Gázquez, J. L.; Vela, A.; Guégan, F.; Chermette, H., Revisiting electroaccepting and electrodonating powers: proposals for local electrophilicity and local nucleophilicity descriptors. *Phys. Chem. Chem. Phys.* **2014,** *16* (48), 26832-26842.
(35) York, D. M.; Yang, W., A chemical potential equalization method for molecular simulations. *J. Chem. Phys.* **1996,** *104* (1), 159-172.
(36) Tognetti, V.; Morell, C.; Joubert, L., Atomic electronegativities in molecules. *Chem. Phys. Lett.* **2015,** *635*, 111-115.
(37) Klein, J.; Fleurat-Lessard, P.; Pilmé, J., New insights in chemical reactivity from quantum chemical topology. *J. Comput. Chem.* **2021,** *42* (12), 840-854.
(38) Klein, J.; Fleurat-Lessard, P.; Pilmé, J., The Topological Analysis of the ELFx Localization Function: Quantitative Prediction of Hydrogen Bonds in the Guanine–Cytosine Pair. *Molecules* **2021,** *26* (11), 3336.
(39) Korchowiec, J.; Uchimaru, T., New energy partitioning scheme based on the self-consistent charge and configuration method for subsystems: Application to water dimer system. *J. Chem. Phys.* **2000,** *112* (4), 1623-1633.
(40) Berkowitz, M., Density functional approach to frontier controlled reactions. *J. Am. Chem. Soc.* **1987,** *109* (16), 4823-4825.
(41) Pilmé, J., Electron localization function from density components. *J. Comput. Chem.* **2017,** *38* (4), 204-210.
(42) Parr, R. G., Companions in the search. *Int. J. Quantum Chem.* **1994,** *49* (5), 739-770.
(43) Wu, Q.; Van Voorhis, T., Constrained Density Functional Theory and Its Application in Long-Range Electron Transfer. *J. Chem. Theory Comput.* **2006,** *2* (3), 765-774.
(44) Ramos, P.; Pavanello, M., Constrained subsystem density functional theory. *Phys. Chem. Chem. Phys.* **2016,** *18* (31), 21172-21178.
(45) Li, C.; Voth, G. A., Using Constrained Density Functional Theory to Track Proton Transfers and to Sample Their Associated Free Energy Surface. *J. Chem. Theory Comput.* **2021,** *17* (9), 5759-5765.
(46) Kaduk, B.; Kowalczyk, T.; Van Voorhis, T., Constrained Density Functional Theory. *Chem. Rev.* **2012,** *112* (1), 321-370.
(47) Wu, Q.; Van Voorhis, T., Direct optimization method to study constrained systems within density-functional theory. *Phys. Rev. A* **2005,** *72* (2), 024502.
(48) Becke, A. D., A multicenter numerical integration scheme for polyatomic molecules. *J. Chem. Phys.* **1988,** *88* (4), 2547-2553.
(49) Herbert, J. M.; Carter-Fenk, K., Electrostatics, Charge Transfer, and the Nature of the Halide–Water Hydrogen Bond. *J. Phys. Chem. A* **2021,** *125* (5), 1243-1256.
(50) Epifanovsky, E.; Gilbert, A. T. B.; Feng, X.; Lee, J.; Mao, Y.; Mardirossian, N.; Pokhilko, P.; White, A. F.; Coons, M. P.; Dempwolff, A. L., et al., Software for the frontiers of quantum chemistry: An overview of developments in the Q-Chem 5 package. *J. Chem. Phys.* **2021,** *155* (8).
(51) Grimme, S.; Ehrlich, S.; Goerigk, L., Effect of the damping function in dispersion corrected density functional theory. *J. Comput. Chem.* **2011,** *32* (7), 1456-1465.
(52) Wu, Q.; Ayers, P. W.; Zhang, Y., Density-based energy decomposition analysis for intermolecular interactions with variationally determined intermediate state energies. *J. Chem. Phys.* **2009,** *131* (16).
(53) Řezáč, J.; de la Lande, A., Robust, Basis-Set Independent Method for the Evaluation of Charge-Transfer Energy in Noncovalent Complexes. *J. Chem. Theory Comput.* **2015,** *11* (2), 528-537.
(54) Chen, C.; Chen, S.-J.; Hong, Y.-S., Comparison of Hydrogen Bonds in FH—CO and FH—OC Weakly Bound Dimer Complexes. *J. Chin. Chem. Soc.* **2005,** *52* (5), 853-861.
(55) Jaffe, R. L.; Smith, G. D., A quantum chemistry study of benzene dimer. *J. Chem. Phys.* **1996,** *105* (7), 2780-2788.

(56) Jurečka, P.; Šponer, J.; Černý, J.; Hobza, P., Benchmark database of accurate (MP2 and CCSD(T) complete basis set limit) interaction energies of small model complexes, DNA base pairs, and amino acid pairs. *Phys. Chem. Chem. Phys.* **2006,** *8* (17), 1985-1993.
(57) Smith, E. L.; Sadowsky, D.; Phillips, J. A.; Cramer, C. J.; Giesen, D. J., A Short Yet Very Weak Dative Bond: Structure, Bonding, and Energetic Properties of N2−BH3. *J. Phys. Chem. A* **2010,** *114* (7), 2628-2636.
(58) Fujimoto, H.; Kato, S.; Yamabe, S.; Fukui, K., Molecular orbital calculations of the electronic structure of borazane. *J. Chem. Phys.* **2003,** *60* (2), 572-578.
(59) Pilme, J.; Silvi, B.; Alikhani, M. E., Structure and Stability of M−CO, M = First-Transition-Row Metal: An Application of Density Functional Theory and Topological Approaches. *J. Phys. Chem. A* **2003,** *107* (22), 4506-4514.
(60) Frenking, G.; Fernández, I.; Holzmann, N.; Pan, S.; Krossing, I.; Zhou, M., Metal–CO Bonding in Mononuclear Transition Metal Carbonyl Complexes. *JACS Au* **2021,** *1* (5), 623-645.
(61) Barone, V., Structure, thermochemistry, and magnetic properties of binary copper carbonyls by a density-functional approach. *J. Phys. Chem.* **1995,** *99* (30), 11659-11666.
(62) Chatt, J.; Duncanson, L. A., 586. Olefin co-ordination compounds. Part III. Infra-red spectra and structure: attempted preparation of acetylene complexes. *J. Chem. Theory Comput.* **1953,** (0), 2939-2947.
(63) Grabowski, S. J., Tetrel bond–σ-hole bond as a preliminary stage of the SN2 reaction. *Phys. Chem. Chem. Phys.* **2014,** *16* (5), 1824-1834.
(64) Fringuelli, F.; Taticchi, A., *The Diels-Alder reaction: selected practical methods*. John Wiley & Sons: 2002.
(65) Pieniazek, S. N.; Clemente, F. R.; Houk, K. N., Sources of Error in DFT Computations of C□C Bond Formation Thermochemistries: π→σ Transformations and Error Cancellation by DFT Methods. *Angew. Chem., Int. Ed.* **2008,** *47* (40), 7746-7749.
(66) Loco, D.; Chataigner, I.; Piquemal, J.-P.; Spezia, R., Efficient and Accurate Description of Diels-Alder Reactions Using Density Functional Theory**. *ChemPhysChem* **2022,** *23* (18), e202200349.
(67) Berski, S.; Andrés, J.; Silvi, B.; Domingo, L. R., The Joint Use of Catastrophe Theory and Electron Localization Function to Characterize Molecular Mechanisms. A Density Functional Study of the Diels−Alder Reaction between Ethylene and 1,3-Butadiene. *J. Phys. Chem. A* **2003,** *107* (31), 6014-6024.
(68) Meyer, B.; Guillot, B.; Ruiz-Lopez, M. F.; Genoni, A., Libraries of Extremely Localized Molecular Orbitals. 1. Model Molecules Approximation and Molecular Orbitals Transferability. *J. Chem. Theory Comput.* **2016,** *12* (3), 1052-1067.